

pubs.acs.org/acsapm Article

Synthesis of PEG and Quaternary Ammonium Grafted Silicone Copolymers as Nanoemulsifiers

Srishti Gupta, Pummy Singh, Babak Moghadas, Bradley J. Grim, Vikram D. Kodibagkar, and Matthew D. Green*



Cite This: https://dx.doi.org/10.1021/acsapm.0c00103



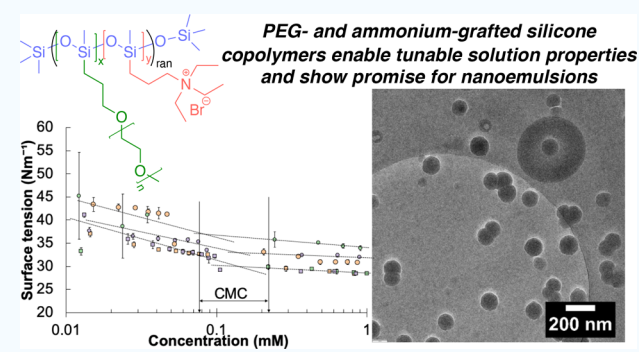
ACCESS

III Metrics & More

Article Recommendations

Supporting Information

ABSTRACT: Amphiphilic silicone copolymers are an exciting class of biomedically relevant polymers that can be used for magnetic resonance imaging (MRI)-based cell labeling and oximetry studies. However, the solution characteristics and the ability to form stable nanoemulsions must be first demonstrated. Therefore, a series of amphiphilic siloxanes were successfully synthesized by grafting allylic poly(ethylene glycol) (PEG) with three (PEG(3)) or 11 (PEG(11)) repeat units or allylic triethylammonium bromide (QUAT) substituents onto polyhydromethylsiloxane backbones at three different PEG:ammonium molar ratios by using a one-pot reaction pathway. The PEG length and the PEG:QUAT molar ratio were varied to tune the hydrophilicity and surface tension, and the polymer structures were confirmed by using ¹H NMR and FT-IR



spectroscopy. The results show that the water contact angle increased upon attaching the PEG and QUAT groups, while the surface tension was most sensitive to the PEG(3) concentration. Also, the critical micelle concentration of the silicone graft copolymers decreased with an increase in the PEG content. Dynamic light scattering (DLS) and cryogenic transmission electron microscopy probed the solution structures and the ability to form nanoemulsions encapsulating polydimethylsiloxane (PDMS) oils. The graft copolymers containing PEG(3) showed consistent sizes by DLS, but the size distribution changed for the PEG(11) samples as the QUAT concentration increased. Finally, the graft copolymers successfully formed stable nanoemulsions containing PDMS with particle sizes that are appropriate for MRI-based cell labeling and oximetry applications.

KEYWORDS: silicone surfactant, graft copolymer, amphiphilic solution assemblies, nanoemulsions

INTRODUCTION

Amphiphilic block polymers have been utilized in numerous commercial applications such as drug delivery vehicles, ^{1–3} surfactants, ^{4–7} water filtration, ^{8,9} and rheology modifiers. ¹⁰ They have also been used in biomedical applications to deliver poorly soluble drugs and as carriers of imaging agents or cell targeting moieties. ^{11–13} In aqueous solutions, the molecules assemble into a variety of structures depending on the volume fractions and lengths of the hydrophobic and hydrophilic components. ¹⁴ Additionally, the solvent interactions and thermal properties of the segments can influence the characteristics and stability of the assemblies. ¹⁵ Significant work has been performed to understand the thermodynamics and kinetics of assembly under a wide range of conditions.

A special class of amphiphilic block polymers are graft copolymers. In this configuration the polymer backbone has oligomeric or polymeric chains, typically hydrophilic, attached to the backbone, which is usually lipophilic. ¹⁶ These copolymers can have multiple configurations, including "T" or "Y" graft copolymers (i.e., a single graft in the center of the backbone), comb-like copolymers (i.e., many grafts uniformly

attached to the polymer backbone), and random graft copolymers (i.e., grafts randomly distributed along the backbone); in each case the graft length can vary significantly.¹⁷ The solution assembly and phase separation behavior of linear amphiphilic block copolymers are driven by the overall chain length and the volume fraction of each block, whereas the architecture of graft copolymers enables the morphology and assembly to be tailored independent of these variables.^{18,19} Also, the synthesis of these molecules deviates from the protocols used to make linear amphiphilic block polymers. Linear amphiphilic block polymers are typically synthesized via sequential addition during living polymerization and less frequently prepared by conjugating two polymers together after the individual segments have been

Received: January 30, 2020 Accepted: April 8, 2020 Published: April 8, 2020



synthesized.^{20–22} Graft copolymers are synthesized by conjugating oligomeric or polymeric fragments to a reactive polymer backbone as well as by growing a polymer graft off the backbone.¹⁷

There are two common classes of graft copolymers: hydrocarbon and silicone graft copolymers. Silicone graft copolymers have a backbone containing siloxane (or -Si-O-Si) bonds, which are more flexible than the C-C bonds present in hydrocarbon surfactants.²³ This flexibility is one reason why silicone polymers can achieve lower surface tensions than hydrocarbon polymers.²⁴ Hydrocarbon surfactants have exhibited surface tensions as low as 30 dyn/cm, whereas silicone surfactants have reduced surface tension to 20 dyn/cm.²⁵ Lowered surface and interfacial tension, superwetting, self-assembly, and aggregation are some of the characteristics of siloxanes which have led to their applications as textiles, fibers, personal care products, cosmetics, and paints and coatings since their first introduction into the market in the 1950s. 25 Having characteristics like other amphiphilic molecules, siloxanes have been considered as either an alternate or add-on to hydrocarbon amphiphiles in various formulations. Because of their increasing use, several assessments have been made to calculate the risk of silicones to human health.²⁶ They have been found to be mostly inert toward living organisms and are considered nontoxic materials. This has led to an increase of their use in pharmaceutical and medical applications as a material of choice for drug delivery applications and implantable devices. 27,28

By themselves, like hydrocarbons, silicones are too hydrophobic to dissolve in polar solvents, but their hydrophilicity is increased by attaching polar groups to the polymer. Polar groups can be nonionic or charged, and the nature of the polar group can tune the properties accordingly. For example, the type of charged group can make the polymer suitable for antimicrobial coatings^{29,30} or give the surfactant the necessary characteristics for cosmetic formulations.³¹ Silicone surfactants have three basic forms: short diblock copolymers (e.g., trisiloxane surfactants that contain three siloxane repeat units linked to a hydrophilic segment), block polymers (e.g., longer AB or ABA block polymers), and graft copolymers.²⁵ These are typically synthesized by using hydrosilylation reactions to graft different functional groups onto the silicone chain.³²

Poly(ethylene glycol) (PEG) and poly(propylene glycol) are nonionic groups often used to increase the hydrophilicity of silicone surfactants.²⁵ This improves the solubility of silicone surfactants in polar solvents and permits solution assemblies to form. Silicones modified with PEG exhibit strong surface activity, and the PEG content impacts the surface tension and hydrophilicity of the silicone surfactant.^{33,34} Recently, siloxanes have been used for tissue oximetry^{35–39} and cell labeling applications.^{40,41} These emerging applications underscore the importance of designing new silicone surfactants that can better solubilize silicone oils than conventional hydrocarbon surfactants to form stable, nontoxic nanoemulsions.

In addition to PEG as a functional group to introduce hydrophilicity, quaternary ammonium salts are cationic molecules that are used in pharmaceutical and personal care product formulations to provide surfactants with antimicrobial activities against bacteria and phytopathogenic fungi. 42 Quaternary ammonium salts have also been shown to increase the hydrophilicity of siloxanes, but to a lesser extent than PEG substituents. 43 Formulations are often based on the hydrophilic—lipophilic balance (HLB) that shifts based on the

fraction of each component; the HLB can affect the shelf life of a product. He is prior work, PEG and quaternary ammonium salts have been grafted individually to silicone backbones. However, it is expected that grafting both quaternary ammonium and PEG moieties onto the silicone backbone will provide HLB tunability and optimization.

Herein, this study probes the effects of simultaneously grafting PEG oligomers of varying length and quaternary ammonium functionalities to a silicone backbone. Specifically, we have synthesized a new series of six silicone graft copolymers containing PEG with 3 or 11 repeat units and quaternary ammonium salts at three PEG:ammonium molar ratios. To our knowledge, this is the first time both PEG and quaternary ammonium salts have been grafted onto a single silicone backbone. Simultaneous addition enhances the ability to modify surfactant characteristics, such as surface tension, hydrophilicity, and the critical micelle concentration. Additionally, though not studied herein, introducing quaternary ammonium functionalities could provide antimicrobial properties to the copolymers, which has been shown in previous studies. 48 Therefore, the hydrophilicity, surface tension properties, and self-assembly of these molecules are detailed in the following report. We also demonstrate application of these molecules as surfactants to form stable nanoemulsions of polydimethylsiloxane (PDMS) in water. PDMS nanoemulsions have recently been used for tissue oximetry and cell labeling^{36,39-41} and may benefit from improved design of siloxane surfactants for emulsification.

■ EXPERIMENTAL SECTION

Materials. Poly(ethylene glycol) monomethyl ether $(M_n 550, PEG(11))$, triethylene glycol monomethyl ether (PEG(3)), Karstedt's catalyst [platinum divinyltetramethyldisiloxane [Pt(dvs)] 3% in xylene solution], allyl bromide, sodium hydride (60% dispersed in mineral oil), triethylamine, chloroform (NMR grade), and D_2O were obtained from Sigma-Aldrich. Poly(hydromethylsiloxane) (PHMS) $(M_n = 1700-3200 \text{ g/mol})$, or 20 repeat units) and polydimethylsiloxane (PDMS, $M_n = 410 \text{ g/mol})$ were obtained from Gelest. The ACS reagent grade solvents diethyl ether, chloroform, tetrahydrofuran (THF), toluene, and acetone were purchased from Fisher Scientific.

Synthesis of Allyl-PEG. The synthesis of allylpoly(ethylene glycol) (allyl-PEG) is described elsewhere. First, 0.06 mol of either PEG(11) or PEG(3) was added dropwise to a suspension of 0.12 mol of NaH in 50 mL of THF under an inert environment. The mixture was maintained at 0 °C for 3 h, following which 0.12 mol of allyl bromide dissolved in 50 mL of THF was added dropwise to the reaction. The temperature was increased to room temperature, and the mixture was stirred for 18 h. The solvent was then removed to yield an orange oil. The product was extracted in chloroform, and solvent was removed under vacuum. Allyl-PEG was obtained as a pale yellow, viscous liquid, and the structure was confirmed by ¹H NMR spectroscopy (Figure S1).

Synthesis of Allyltriethylammonium Bromide (QUAT). The synthesis of allyltriethylammonium bromide (QUAT) is described elsewhere. ⁴⁵ Herein, 0.05 mol of allyl bromide was added to a solution of triethylamine (0.07 mol) in acetonitrile (70 mL) in a round-bottomed flask equipped with reflux condenser and stir bar. The solution was maintained at 50 °C for 10 h. The product was precipitated in diethyl ether. The precipitate was filtered and dried under vacuum, and the structure was confirmed by ¹H NMR spectroscopy (Figure S2).

Synthesis of Graft Copolymer Siloxanes. First, 0.05 mmol of PMHS was dissolved in 10 mL of toluene and then placed in a two-neck, round-bottomed flask equipped with a reflux condenser and a rubber septum along with the desired quantities of allyl-PEG and QUAT. The reaction was run under inert conditions by purging with

nitrogen. The contents of the reactor were mixed for 15 min, and the reactor temperature was raised to 75 °C. Then, 250 μ L of Pt(dvs) catalyst was added to the mixture. Because the reaction is exothermic, a slight effervescence was observed upon adding the catalyst. The reaction was run for 18 h under reflux. The residual reactants were removed by using dialysis in THF, and the final product was dried under vacuum. The polymer structure was characterized by using 1 H NMR spectroscopy and Fourier transform infrared spectroscopy (FT-IR).

Characterization. ¹H NMR spectra were obtained by using a Bruker FT-NMR spectrometer (400 MHz) with CDCl₃ or D₂O as the solvent. ¹H NMR spectroscopy samples were prepared by dissolving 20–22 mg of polymer in solvent. All of the samples prepared were clear solutions and free from suspended dust and impurities. These samples were injected into clean, dry NMR tubes.

A Bruker IFS66 V/S FT-IR/FT-Raman instrument was used to obtain the ATR-FTIR spectrum at room temperature in the range 4000–400 cm⁻¹. The sample was mounted over the diamond, and the spectra were obtained under vacuum (<5 mbar). Each reported spectrum is the average of 32 scans.

Physical Property Characterization. A thin layer of the polymers on glass slides was obtained by using a VTC-100 vacuum spin coater for contact angle measurements. 0.05 g of each sample was dissolved in 0.66 g of THF and spin-coated at 4000 rpm for 120 s. Static contact angle measurements were performed using a ramè-hart contact angle goniometer installed with an automatic water dispenser, video camera, and drop analysis software. The angle was measured by calculating contact angle made by 5 μ L sessile drop of water on the glass slide after 30 s. The reported angles are an average of four measurements taken at different areas of each sample.

Surface Tension. First, 10 mg of each sample was dissolved in 2 mL of distilled water to make a stock solution for surface tension measurements. Aqueous solutions were used to analyze the air—water interfacial tension using a ramè-hart tensiometer installed with an automatic water dispenser, video camera, and drop analysis software. The surface tension was obtained by fitting the Young—Laplace equation to the contour profile of a 5 μ L water drop 120 s after it formed at the tip of the syringe needle. The contour fitting assumes a characteristic shape and size, which is used to calculate surface tension. These conditions resulted in average Bond numbers >0.2 for all samples (Table S1), which should limit the dependence of surface tension on the testing parameters. So Surface tension was calculated by taking the average of three surface tension measurements, each after waiting 100—120 s.

Nanoemulsion Formulation. PDMS-based nanoemulsions (20 vol % PDMS) were prepared by using the synthesized graft copolymers as surfactants using a procedure used before. Briefly, 4 mL of deionized water was heated to 60 °C, and then a calculated amount of the polymers (2 wt %) was added. Next, 1 mL of PDMS was added dropwise to the mixture and stirred while heating for 15 min. Then, the mixture was sonicated with a probe sonicator three times at 15 min intervals. Finally, the emulsion was filtered 11 times through a filter with pore sizes of 0.22 μ m. To assess the particle size, DLS was performed on the final mixture.

Dynamic Light Scattering (DLS). DLS was used to determine the polymer size in solution as well as to determine the size of nanoemulsions formed by using these polymers as emulsifiers. For estimating polymer size, 5 mg of each siloxane sample was dissolved in 1 mL of water. The analysis was done by using a Zetasizer Nano ZS equipped with a He–Ne laser operating at a wavelength of 633 nm. The experiment was done at 25 °C with 120 s equilibration time and 173° scattering angle. The data processing was done by compiling CONTIN^{51–53} in MATLAB using code from Marino⁵⁴ that was optimized by L-curve criteria using code from Hansen. ⁵⁵

For estimating the nanoemulsion size, a DelsaNano DLS system (Beckman Coulter) was used. The nanoemulsion sample, as prepared, was diluted 50× for the measurement. Measurements were performed over 7 h to assess the stability of particles. Number-average particle sizes are reported.

Cryogenic Transmission Electron Microscopy. Carbon-coated copper (Quantifoil R 2/1) grids were plasma cleaned for 60 s and transferred to a FEI Vitrobot Mk IV (version 2.14.1219) held at 25 °C and 100% relative humidity. Samples were prepared by diluting $100\times$ by volume from the stock solutions described in the previous section. A 4 μ L aliquot of each was pipetted consecutively onto each respective grid inside the Vitrobot. Excess liquid was removed by blotting once with filter paper, blot time (6 s), wait time (1 s), blot force (0 (on a relative scale from -25 to 25)), and drain time (0 s). The sample was then plunged into liquid ethane and stored in liquid nitrogen before imaging. Imaging was performed on a Tecnai F20 operating at a high tension of 200 kV. Images were collected by using a Teitz XF417F camera while using a nominal underfocus to improve contrast. The microscope and Gatan CT3500 grid holder were kept cool with liquid nitrogen while imaging.

RESULTS AND DISCUSSION

Synthesis and Structural Characterization of PEG and Ammonium Grafted Silicone Copolymers. The PEG- and QUAT-modified silicone graft copolymers were synthesized according to a multistep synthetic protocol (Scheme 1). First,

Scheme 1. Synthesis of PHMS-g-PEG $(n)_x$ -g-QUAT $_y$ by Simultaneously Grafting PEG(n) and QUAT at Different Ratios (x:y) onto PHMS a

PHMS
$$x \downarrow O \downarrow_{nO} \qquad PEG_{n}$$

$$pEG_{n} \qquad PEG_{n}$$

$$QUAT$$

$$pHMS-g-PEG(n)_{x}-g-QUAT_{y}$$

$$pHMS-g-PEG(n)_{x}-g-QUAT_{y}$$

 a The PHMS, PEG(n), and QUAT refer to polyhydromethylsiloxane, allyl poly(ethylene glycol), and allyltriethylammonium bromide, respectively.

allyl-PEG and allyl-QUAT were synthesized by $S_{\rm N}2$ substitution reactions. PEG chains of two lengths were reacted with allyl bromide in the presence of sodium hydride, whereas trimethylamine and allyl bromide required only heat to react. Excess allyl bromide was added to both reactions to ensure complete conversion to allyl-PEG or allyl-QUAT. The structures of allyl-PEG(11), allyl-PEG(3), and allyl-QUAT were analyzed by using $^1{\rm H}$ NMR spectroscopy. The $^1{\rm H}$ NMR spectra of all the allyl-containing species (Figures 1ii and 1iii) show the peaks of the starting material, peaks from unsaturated bonds at 5.58 and 5.15 ppm, and peaks from the allylic CH₂ linker at 3.95 ppm, thus confirming the addition of allyl group to the structure.

The hydrophilic, allyl-containing compounds were grafted onto the siloxane backbone by using the hydrosilylation reaction (Scheme 1). Hydrosilylation reactions are often hampered by competing side reactions including hydrogenation, isomerization, oligomerization, and redistributions. Also, Si–H bonds can be hydrolyzed by moisture forming silanol and hydrogen gas, which reduce the functionality. Because the rate of the catalyzed hydrosilylation is fast relative to the side reactions, an excess of the allyl-containing compounds was fed to reduce the formation of undesirable

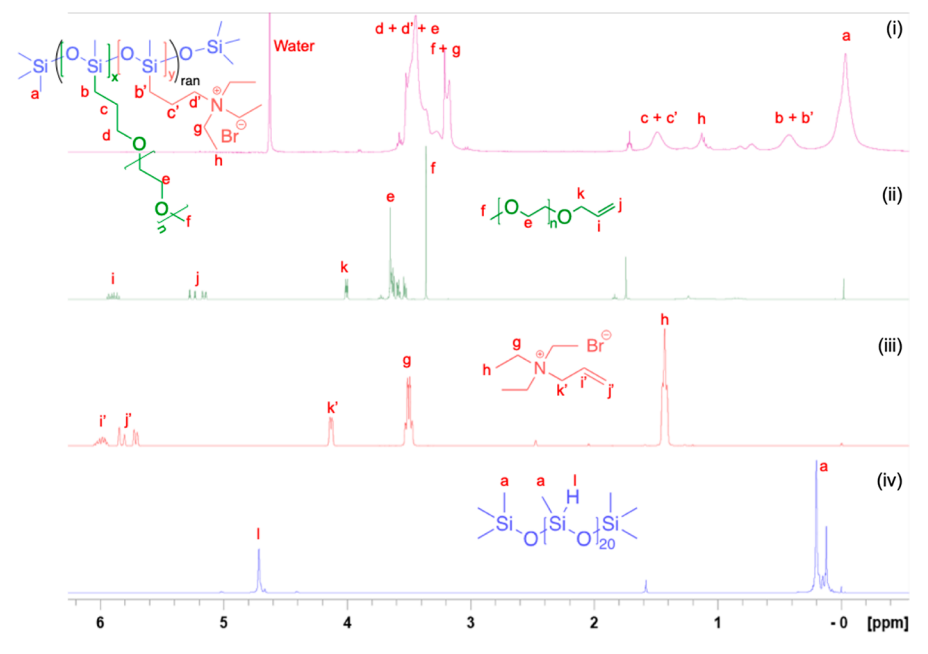


Figure 1. Representative ¹H NMR spectra of (i) PHMS-g-PEG(11)₁₀-g-QUAT₁₀, (ii) allyl-PEG, (iii) allyltriethylammonium bromide, and (iv) PHMS.

products. The structures of the final products were analyzed by using 1H NMR spectroscopy. The peaks in the 1H NMR spectra at 0 and 4.7 ppm represent the protons of the Si–CH $_3$ methyl group and the proton of the Si–H silane group, respectively (Figure 1iv). The absence of the Si–H peak in the final product (Figure 1i) confirms complete conversion of the silane group to the grafted allyl groups.

After the synthesis conditions were validated, two series of polymers were prepared. The ratio of PEG:QUAT was varied, and the length of the PEG was also varied. The molar ratio of PEG:QUAT was kept constant between the two PEG lengths. 1 H NMR spectroscopy was used to obtain the actual molar ratios of PEG (x, PHMS:PEG) and QUAT (y, PHMS:QUAT). The original PHMS siloxane possessed \sim 20 silane groups, and complete conversion of these groups was targeted and obtained; thus, the subscripts denoting the mole fraction of PEG and QUAT sum to 20 and denote the mole fractions of PEG:QUAT. The data are summarized in Table 1. Higher values of y were targeted, but the resulting polymers displayed limited solubility, which was indicative of chemical cross-linking; thus, further investigation into these materials

Table 1. Quantitative ¹H NMR Spectroscopy Analyses for the Siloxane Graft Copolymers with PEG:QUAT $\equiv x:y$

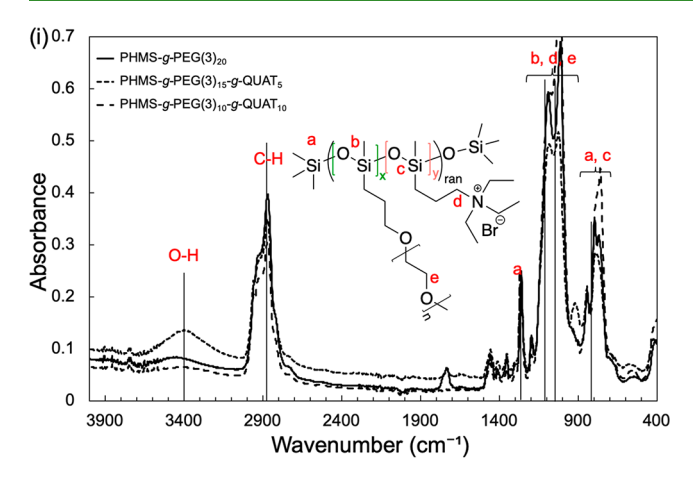
	target		obtained			
	x	у	x	у	(n)	$M_{\rm n} ({ m g/mol})$
PHMS-g-PEG $(3)_{20}$	20	0	20	0	3.2	4178
PHMS- g -PEG(3) ₁₅ - g -QUAT ₅	15	5	13.8	6.2	3.2	4694
PHMS- g -PEG(3) ₁₀ - g -QUAT ₁₀	10	10	12	8	3.2	4844
PHMS- g -PEG(11) ₂₀	20	0	20	0	11.1	11130
PHMS-g-PEG(11) ₁₅ -g- QUAT ₅	15	5	13.3	6.7	11.1	9359
PHMS-g-PEG(11) ₁₀ -g- QUAT ₁₀	10	10	12.4	7.6	11.1	9121

was abandoned. Overall, the relative agreement between the targeted mole fraction and the obtained mole fraction and the quantitative agreement between the PHMS backbone and the PEG or QUAT grafts suggest that the formation of unwanted side products does not occur at an appreciable rate.

A qualitative analysis of the samples was done by using FT-IR spectroscopy to better understand the structural composition of the synthesized polymers. Characteristic peaks for $-\text{Si}(\text{CH}_3)-\text{O-}$, $-\text{Si}-\text{CH}_2-$, and -Si-O-Si were identified in the spectra (Figure 2). The Si-H peak (2000–2150 cm⁻¹) was not present in any of the final product spectra, corroborating earlier evidence for complete conversion of the Si-H group during the hydrosilylation reaction. Because of peak overlaps, the molar ratios of different grafted substituents could not be quantified; however, the FTIR spectra support the ¹H NMR spectroscopy data.

The silicone precursor polymers are very hydrophobic; thus observing a change in the hydrophobicity is a facile method to further confirm the structural changes noted above. Specifically, measuring the water contact angle of the various polymers would determine the effect that the PEG chain length and PEG concentration (relative to QUAT) in the copolymer would have on the hydrophilicity of the polymers. An overall increase in the PEG composition was expected to increase the hydrophilicity of the polymer. PHMS serves as the hydrophobic control with a contact angle of ~85°. As predicted, we observe that grafting hydrophilic side chains significantly reduces the contact angle of the graft copolymer siloxanes (Figure 3). The water contact angle of PEG grafted siloxanes is comparable to values found in the literature. ⁵⁷ It was also observed that the contact angles further reduce upon grafting the QUAT salts. Increasing the chain length from PEG(3) to PEG(11) did not have any significant effect on the water contact angle of the material.

Characterization of Ammonium and PEG Grafted Copolymer Surface Tension and Micellization. Next, the ability of the graft copolymers to act as surfactants was studied by measuring the surface tension of polymer solutions at



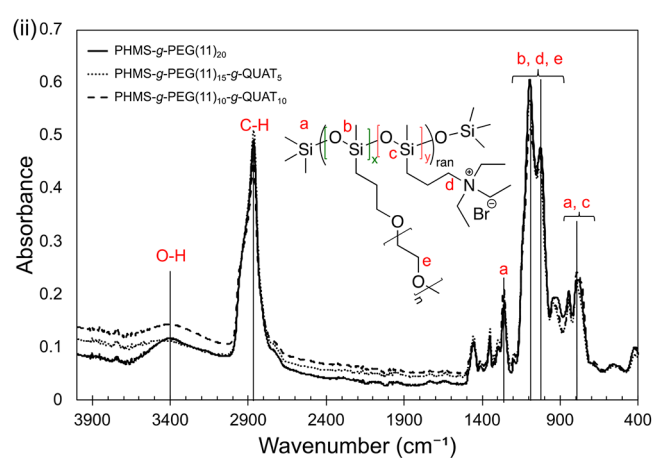


Figure 2. ATR-FTIR spectra of (i) PHMS-g-PEG(3)_x-g-QUAT_y and (ii) PHMS-g-PEG(11)_x-g-QUAT_y.

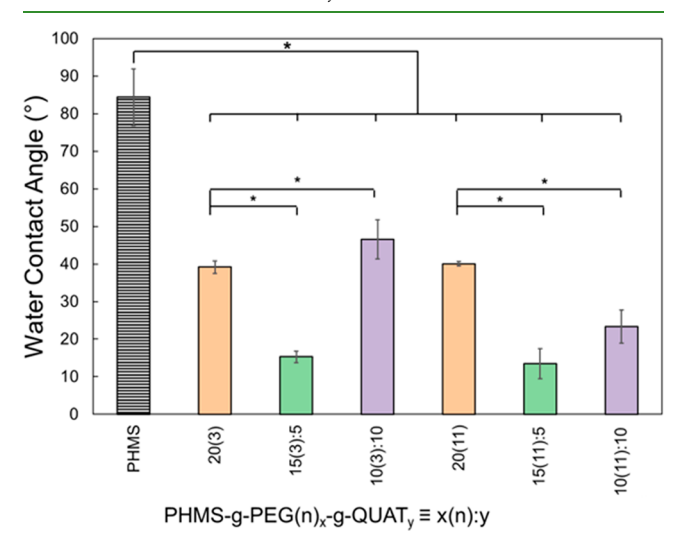


Figure 3. Static water contact angle for the synthesized graft copolymer siloxanes (PHMS-g-PEG(n) $_y$ -g-QUAT $_z$). PHMS is used as a control. The student's t test confirmed that the PEG:QUAT ratio significantly affects the hydrophilicity of the graft copolymer siloxanes (* indicates p < 0.05).

different concentrations. In this experiment the surface tension, or air—water interfacial tension, of the polymer solutions was measured by using the pendant drop method. Figure 4 shows the equilibrium surface tension in a 5 μ L droplet plotted against the natural log of the concentration. The surface

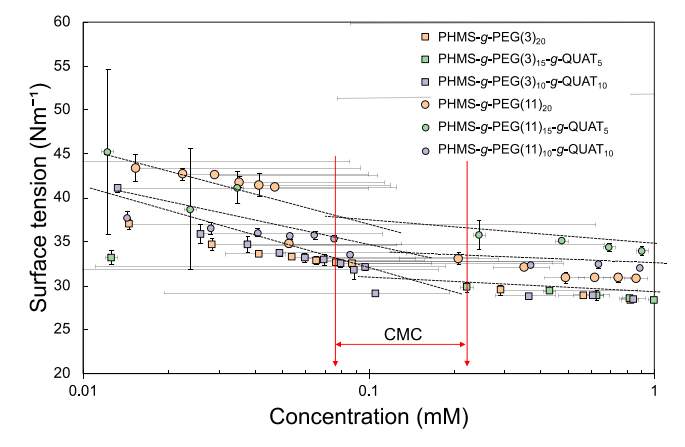


Figure 4. Dependence of surface tension on polymer concentration for the PEG and ammonium grafted siloxane copolymers.

tension reached equilibrium after 80 s (Figure S3), and all measurements were taken between 100 and 120 s after droplet formation. The Bond number for all the samples was between 0.2 and 0.3 (Table S1), which indicates that the surface tension reported should be independent of testing parameters, such as needle diameter and droplet volume. 50 The graft copolymers with the longer PEG(11) substituent have a higher surface tension when compared to the graft copolymers with the PEG(3) substituent. These results are comparable to previous studies that describe the effect of poly(ethylene oxide) on surface tension of polydimethylsiloxane. 46 The effect of adding the QUAT was dependent on the PEG substituent length. For the PEG(3) series, the addition of the quaternary ammonium did not impact the surface tension of the samples above or below CMC. For the PEG(11) series, the surface tension increased from PHMS-g-PEG(11)₂₀ to PHMS-g-PEG(11)₁₅-g-QUAT₅ but then decreased upon further addition of the ammonium group to PHMS-g-PEG(11)₁₀-g-QUAT₁₀ (Table 2). Also, the surface tension for PHMS-g-PEG(11)₁₀-g-

Table 2. Surface Tension and Critical Micelle Concentrations of PHMS-g-PEG $(n)_x$ -g-QUAT $_y$

	surface tension $(mN \ m^{-1})$	CMC (mM)
PHMS- g -PEG(3) ₂₀	28.3 ± 0.5	0.165
PHMS- g -PEG(3) ₁₅ - g -QUAT ₅	28.5 ± 0.4	0.090
PHMS- g -PEG(3) ₁₀ - g -QUAT ₁₀	28.8 ± 0.3	0.125
PHMS-g-PEG $(11)_{20}$	30.9 ± 0.0	0.080
PHMS-g-PEG(11) ₁₅ -g-QUAT ₅	33.1 ± 0.3	0.068
PHMS- g -PEG(11) ₁₀ - g -QUAT ₁₀	32.2 ± 0.2	0.091

QUAT $_{10}$ was higher than PHMS-g-PEG $(11)_{20}$. These data suggest that the PEG chain length has a strong influence on the surface activity of the surfactant as well as that the QUAT salt has an influence on the surface activity though it is more complex.

Critical micelle concentrations (CMCs) are also determined from Figure 4, which are taken as the intersection of the two straight lines of surface tension at high and low concentrations. For the graft copolymer siloxanes, we observed that the CMC for all the surfactants is between 0.068 and 0.165 mM (or 0.3 to 1.0 g/L), which is comparable to surfactants present in the literature. The siloxanes grafted with PEG(11) tended to reach the minimum surface tension faster than siloxanes with PEG(3), indicating that chain length of the ethylene glycol

oligomer is the principal factor for reducing the CMC. For both series, the CMC decreases upon adding QUAT from PHMS-g-PEG(11) $_{20}$ to PHMS-g-PEG(11) $_{15}$ -g-QUAT $_{5}$. However, it again decreases upon increasing QUAT content from PHMS-g-PEG(11) $_{15}$ -g-QUAT $_{5}$ to PHMS-g-PEG(11) $_{10}$ -g-QUAT $_{10}$. The CMC depends upon various factors like micelle size, aggregation number, micelle shape, and monomermicelle equilibrium. For additional clarity, the surface tension values are plotted against a linear concentration axis in Figure S4, which shows the consistency in surface tension above the reported CMCs. The surface tension would continue to decrease if a critical aggregation concentration had been obtained. 59

The surface tension data were compared to a literature report that prepared a series of PEG-PHMS graft copolymers. Chung and co-workers studied the effects of PEG graft length, PEG content, and the PHMS chain length.⁴⁶ They observed that the PEG length and PEG content increased the surface tension when the PHMS chain was held constant. A similar result for PEG length is reported herein. Additionally, they noted that when the PEG content and PHMS chain length were varied (i.e., constant PEG length), the PHMS chain length dominated the surface tension effects. Finally, when the PEG and PHMS lengths were fixed, the PEG content did not greatly affect the surface tension. These data, together with the prior report that ammonium grafts do not affect the hydrophilicity as profoundly as PEG,⁴³ corroborate our findings that increasing ammonium content modestly increases the surface tension.

Based on the size and length of hydrophobic and hydrophilic parts of surfactants, the micelle aggregates can take up several morphologies, such as spheres, cylinders, or bilayers. 19 No relation between molecular structure and morphology has been found in the literature for amphiphilic siloxanes. This is because siloxane chains tend to coil due to the flexibility of the backbone; therefore, the thickness of aggregates is much smaller than the extended molecular chain length. Dynamic light scattering (DLS) experiments were performed to estimate the size of the siloxane graft copolymers at concentrations above the CMCs. The average particle sizes, standard deviations, and polydispersity indices were assessed from the intensity distribution profiles (Figure 5). Recall that for DLS low values of polydispersity index (approaching 0) indicate a monomodal and narrow size distribution, whereas high values (approaching 1.0) indicate a broad or multimodal size distribution leading to difficulty in data analysis. Generally, the shorter PEG substituent resulted in smaller particle sizes, and increasing the fraction of QUAT substituents seemed to have no consistent effect. For comparison, the particle sizes, standard deviations, and polydispersity indices from the intensity distribution profile (Table S2) and number distribution profile are provided in the Supporting Information (Table S3). Additionally, autocorrelation curves are presented (Figure S5) due to the dispersity in size that was observed, which reduced confidence in the sizes and size distributions reported. It is useful to recall, when analyzing these plots, that the autocorrelation curve will decay quickly for smaller particles. As the size of the aggregates increases, the correlation curve decays further away from origin. From Figure S5a, the size of aggregates is almost the same for all of the PEG(3) graft copolymers and does not depend on QUAT content in the final product. This is consistent with the particle sizes from the intensity distribution. However, Figure S5b shows that as the

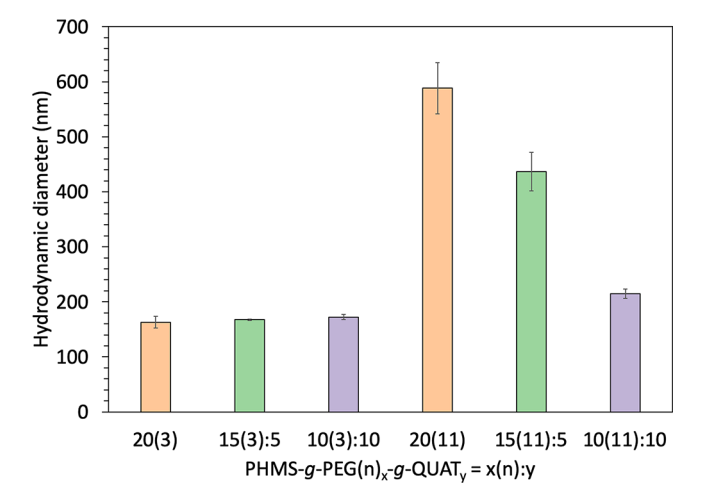


Figure 5. Hydrodynamic diameter results obtained via the intensity distribution profiles from dynamic light scattering for PEG- and ammonium-grafted silicone copolymers (PHMS-g-PEG(n) $_x$ -g-QUAT $_v$).

PEG(11) content increases in the final product, the autocorrelation curve decays at a longer correlation time. Moreover, the curve displays two plateaus, which is indicative of a bimodal distribution of particles. The second distribution has a larger size than any of the PEG(3) graft copolymers. The intensity distribution sizes for the PEG(11) copolymer with the highest QUAT content (i.e., PHMS-g-PEG(11) $_{10}$ -g-QUAT $_{10}$) are similar to the PEG(3) copolymers, which is reflected in the similar decay time seen in the autocorrelation plot. Similarly, the larger average sizes from the intensity distributions in Figure 5 are consistent with the bimodal distribution. Therefore, the chain length of PEG plays an important role in deciding the size, modality (i.e., monomodal vs multimodal), and size distribution of the aggregates.

Characterization of Formation and Stability of PDMS Nanoemulsions. The feasibility of formulating nanoemulsions containing PDMS was tested for the three PEG(11) surfactants. DLS measurements were performed over a period of 97 h to monitor any changes in the particle size. DLS data (Figure 6) confirmed the generation of nanoemulsions from all

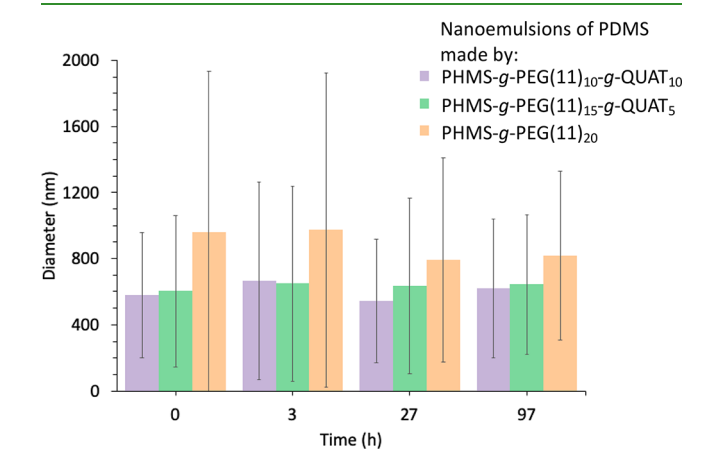


Figure 6. Dynamic light scattering (DLS) data for particle size estimation of nanoemulsions from intensity distribution profiles, wherein polydimethylsiloxane ($M_{\rm n}$ = 410 g/mol) was emulsified using PHMS-g-PEG(11)₂₀, PHMS-g-PEG(11)₁₅-g-QUAT₅, and PHMS-g-PEG(11)₁₀-g-QUAT₁₀.

the three polymers. The nanoemulsion particles all showed a larger diameter relative to the corresponding copolymer (e.g., Figure 6 vs Figure 5). The results did not show any significant difference in size for the three nanoemulsions; however, the mean particle diameter decreased with an increasing QUAT mole fraction. After 97 h, there was no phase separation observed in the nanoemulsions and there was no statistically significant change in nanoemulsion size with respect to time, which suggests the graft copolymers effectively encapsulated the PDMS and the emulsions were stable. For comparison, the particle sizes from the number distribution profile (Figure S6) as well as the autocorrelation curves (Figure S7) for the nanoemulsions are included in the Supporting Information. The autocorrelation curves are consistent with a larger and broader size distribution compared to the copolymer data (e.g., Figure S5b vs Figure S7).

Shown in Figure 7 are the cryo-transmission electron micrographs for the PEG(11) series nanoemulsions with

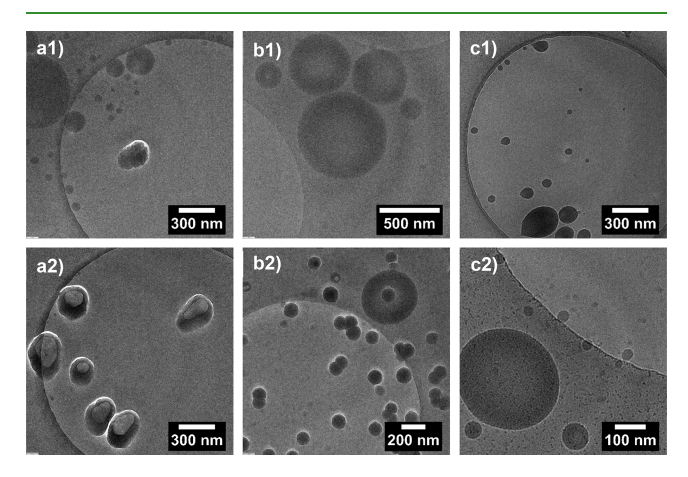


Figure 7. Cryogenic transmission electron microscopy data for nanoemulsions wherein PDMS ($M_{\rm n}=410~{\rm g/mol}$) was emulsified using (a) PHMS-g-PEG(11)₁₀-g-QUAT₁₀, (b) PHMS-g-PEG(11)₁₅-g-QUAT₅, and (c) PHMS-g-PEG(11)₂₀.

decreasing QUAT content (a > b > c). The micellar elongation observed in Figure 7c1 is attributed to shear forces exerted on the sample during preparation. The sample containing the greatest QUAT content exhibits two different formations of equivalent size (Figures 7a1 and 7a2). In contrast to the highly spherical nanoemulsions seen in the upper left of Figure 7a1, the structures in Figure 7a2 show bulky, liposomal-like structures which lack a well-defined geometry. This stark difference in morphological states is reduced upon decreasing the QUAT content (Figures 7b and 7c). Two distinct states are still observed, one being highly spherical (Figure 7b1) while the other is depicted by a slightly aberrated surface. These aberrated spheres which comprise most of the formations in Figure 7b2 are small (consistent with DLS data in Figure 6) with an ideal polydispersity. This was consistent across several micrographs of this sample. The deformed particles in the nanoemulsion samples of PHMS-g- $PEG(11)_{10}$ -g-QUAT₁₀ (Figure 7a) and PHMS-g-PEG(11)₁₅-g-QUAT₅ (Figure 7b) appear to lack fluidity and have rough surfaces, which potentially suggests that they do not contain a significant amount of PDMS and instead are large surfactant aggregates. This may represent equilibria from structures formed via undesired side reactions.

The data in Figures 6 and 7 suggest promise for PEG and ammonium grafted silicone copolymers to form stable nanoemulsions. In prior work, a series of gemini siliconebased surfactants were prepared and used to emulsify olive oil.⁴⁷ They synthesized a pentablock terpolymer with a silicone midblock, PEO spacer blocks, and short variable-length hydrocarbon outer blocks. The CMC showed a parabolic trend with the hydrocarbon length as longer hydrocarbon tails began to interfere with micelle formation. The gemini surfactant successfully emulsified olive oil, but the particles were all >1 μ m according to DLS. Recent work highlighted the need for siloxane-based magnetic resonance probes and new emsulsifiers to form stable nanoemulsions containing siloxanes, which can be used for oximetry and cell labeling in vivo, respectively. 36,40,41 However, the spin-lattice relaxation times of ¹H resonances can be very long under hypoxic conditions, which suggests alternative probes are needed;³⁹ specifically, longer siloxane chains (instead of the shorter siloxanes used in early work) and improvements in amphiphilicity can potentially improve temporal sensitivity. Siloxane nanoemulsions have been used for oximetry as well as cell labeling and are advantageous because of the use of ¹H MRI and dual functionality (detection and oximetry). Thus, the ability to tailor the surface tension and CMC of the PEG and ammonium grafted silicone copolymer to form improved nanoemulsions suggests potential in biomedical applications.

CONCLUSIONS

A series of amphiphilic siloxanes were successfully synthesized by hydrosilylation reactions. PEG substituents of two lengths and a QUAT substituent were grafted onto a siloxane backbone through a one-pot reaction pathway at various molar ratios to prepare six novel silicone graft copolymers. ¹H NMR and FT-IR spectroscopy were used for structural analysis of siloxanes. The effects of changing chain length and molar ratios of PEG:QUAT on physical properties were studied. Analysis of the water contact angle showed a relative increase in hydrophilicity upon attaching the polar groups. Surface tension analysis showed that the PEG(3) substituent lowered the surface tension the most. Additionally, the CMC of the silicone graft copolymers decreased with an increase in the PEG content substituted on the surfactant. DLS showed that the structure and size distribution of micelles were consistent for the PEG(3) samples. However, the size distribution changed for the PEG(11) samples as the QUAT concentration increased. The findings presented in this work provide evidence that varying the grafted ratio of PEG:QUAT along the same backbone can be used to tune hydrophilicity, while varying the length of the PEG substituent controls, to a greater extent, the CMC and surface tension behavior. Finally, these amphiphilic polymers allowed the formation of stable PDMS nanoemulsions with particle sizes, based on DLS and cryo-TEM, appropriate for MRI-based cell labeling and oximetry applications. Future studies will focus on cytotoxicity and cell uptake of these nanoemulsions as well as characterization of oxygen sensitivity.

ASSOCIATED CONTENT

Supporting Information

The Supporting Information is available free of charge at https://pubs.acs.org/doi/10.1021/acsapm.0c00103.

Bond numbers from surface tension experiments, ¹H NMR spectra of the allyl-PEG and allyltriethylammonium bromide, time-dependent surface tension data, hydrodynamic diameters from number distribution profiles and intensity distribution profiles for DLS data for copolymers and nanoemulsions, and autocorrelation coefficient plots from DLS for copolymers and nanoemulsions (PDF)

AUTHOR INFORMATION

Corresponding Author

Matthew D. Green — Department of Chemical Engineering, School for Engineering of Matter, Transport and Energy, Arizona State University, Tempe, Arizona 85287, United States; orcid.org/0000-0001-5518-3412; Email: mdgreen8@asu.edu

Authors

Srishti Gupta — Department of Chemical Engineering, School for Engineering of Matter, Transport and Energy, Arizona State University, Tempe, Arizona 85287, United States

Pummy Singh — Department of Chemical Engineering, School for Engineering of Matter, Transport and Energy, Arizona State University, Tempe, Arizona 85287, United States

Babak Moghadas — School of Biological and Health Systems Engineering, Arizona State University, Tempe, Arizona 85287, United States

Bradley J. Grim — Department of Chemical Engineering, School for Engineering of Matter, Transport and Energy, Arizona State University, Tempe, Arizona 85287, United States

Vikram D. Kodibagkar — School of Biological and Health Systems Engineering, Arizona State University, Tempe, Arizona 85287, United States

Complete contact information is available at: https://pubs.acs.org/10.1021/acsapm.0c00103

Notes

The authors declare no competing financial interest.

■ ACKNOWLEDGMENTS

This work was supported in part by funds through the 2019 ASU-Mayo Seed Grant, the 2018 Mayo Clinic and ASU Alliance for Health Care Summer Residency Fellowship, NIH UF1NS107676, NSF CAREER Award 1351992, and NSF CAREER Award 1848454.

REFERENCES

- (1) Dwarakanadha Reddy, P.; Swarnalatha, D. Recent Advances in Novel Drug Delivery Systems; Vol. 2.
- (2) Lukyanov, A. N.; Torchilin, V. P. Micelles from Lipid Derivatives of Water-Soluble Polymers as Delivery Systems for Poorly Soluble Drugs. *Adv. Drug Delivery Rev.* **2004**, *56* (9), 1273–1289.
- (3) Rösler, A.; Vandermeulen, G. W. M.; Klok, H.-A. Advanced Drug Delivery Devices via Self-Assembly of Amphiphilic Block Copolymers. *Adv. Drug Delivery Rev.* **2012**, *64*, 270–279.
- (4) Alexandridis, P. Poly(Ethylene Oxide)/Poly(Propylene Oxide) Block Copolymer Surfactants. *Curr. Opin. Colloid Interface Sci.* 1997, 2 (5), 478–489.
- (5) Davis, M. E.; Tsapatsis, M. On the Origins of Morphological Complexity in Block Copolymer Surfactants. *Angew. Chem., Int. Ed.* **2002**, DOI: 10.1126/science.1082169.
- (6) Alexandridis, P. Amphiphilic Copolymers and Their Applications. Curr. Opin. Colloid Interface Sci. 1996, 1 (4), 490–501.

- (7) Förster, S.; Antonietti, M. Amphiphilic Block Copolymers in Structure-Controlled Nanomaterial Hybrids. *Adv. Mater.* **1998**, *10* (3), 195–217.
- (8) Asatekin, A.; Mayes, A. M. Oil Industry Wastewater Treatment with Fouling Resistant Membranes Containing Amphiphilic Comb Copolymers. *Environ. Sci. Technol.* **2009**, 43 (12), 4487–4492.
- (9) Howarter, J. A.; Youngblood, J. P. Amphiphile Grafted Membranes for the Separation of Oil-in-Water Dispersions. *J. Colloid Interface Sci.* **2009**, 329 (1), 127–132.
- (10) Riess, G.; Hurtrez, G.; Bahadur, P. In Encyclopedia of Polymer Science and Engineering; Mark, H. F., Kroscwitz, J. I., Eds.; Wiley: New York, 1985.
- (11) Kelley, E. G.; Albert, J. N. L.; Sullivan, M. O.; Epps, T. H., III Stimuli-Responsive Copolymer Solution and Surface Assemblies for Biomedical Applications. *Chem. Soc. Rev.* **2013**, 42 (17), 7057–7071.
- (12) Kabanov, A. V.; Alakhov, V. Y. Pluronic® Block Copolymers in Drug Delivery: From Micellar Nanocontainers to Biological Response Modifiers. *Crit. Rev. Ther. Drug Carrier Syst.* **2002**, *19* (1), 1.
- (13) Ryu, J.-H.; Roy, R.; Ventura, J.; Thayumanavan, S. Redox-Sensitive Disassembly of Amphiphilic Copolymer Based Micelles. *Langmuir* **2010**, *26* (10), 7086–7092.
- (14) Ramanathan, M.; Shrestha, L. K.; Mori, T.; Ji, Q.; Hill, J. P.; Ariga, K. Amphiphile Nanoarchitectonics: From Basic Physical Chemistry to Advanced Applications. *Phys. Chem. Chem. Phys.* **2013**, *15* (26), 10580.
- (15) Lombardo, D.; Kiselev, M. A.; Magazù, S.; Calandra, P. Amphiphiles Self-Assembly: Basic Concepts and Future Perspectives of Supramolecular Approaches. *Adv. Condens. Matter Phys.* **2015**, 2015, 1–22.
- (16) Pispas, S.; Hadjichristidis, N.; Mays, J. W. Micellization of Model Graft Copolymers of the H and π Type in Dilute Solution. *Macromolecules* **1996**, 29 (23), 7378–7385.
- (17) Jenkins, D. W.; Hudson, S. M. Review of Vinyl Graft Copolymerization Featuring Recent Advances toward Controlled Radical-Based Reactions and Illustrated with Chitin/Chitosan Trunk Polymers. *Chem. Rev.* **2001**, *101* (11), 3245–3274.
- (18) Pochan, D. J.; Gido, S. P.; Pispas, S.; Mays, J. W.; Ryan, A. J.; Fairclough, J. P. A.; Hamley, I. W.; Terrill, N. J. Morphologies of Microphase-Separated A2B Simple Graft Copolymers. *Macromolecules* **1996**, 29 (15), 5091–5098.
- (19) Jain, S.; Bates, F. S. On the Origins of Morphological Complexity in Block Copolymer Surfactants. *Science (Washington, DC, U. S.)* **2003**, 300 (5618), 460 LP-464.
- (20) Hillmyer, M. A.; Bates, F. S. Synthesis and Characterization of Model Polyalkane— Poly (Ethylene Oxide) Block Copolymers. *Macromolecules* **1996**, 29 (22), 6994—7002.
- (21) Mühlebach, A.; Gaynor, S. G.; Matyjaszewski, K. Synthesis of Amphiphilic Block Copolymers by Atom Transfer Radical Polymerization (ATRP). *Macromolecules* **1998**, *31* (18), 6046–6052.
- (22) York, A. W.; Kirkland, S. E.; McCormick, C. L. Advances in the Synthesis of Amphiphilic Block Copolymers via RAFT Polymerization: Stimuli-Responsive Drug and Gene Delivery. *Adv. Drug Delivery Rev.* **2008**, *60* (9), 1018–1036.
- (23) Hill, R. M. Silicone Surfactants—New Developments. *Curr. Opin. Colloid Interface Sci.* **2002**, 7 (5–6), 255–261.
- (24) Ananthapadmanabhan, K. P.; Goddard, E. D.; Chandar, P. A Study of the Solution, Interfacial and Wetting Properties of Silicone Surfactants. *Colloids Surf.* **1990**, *44*, 281–297.
- (25) Hill, R. M. Silicone Surfactant; 1999.
- (26) Mojsiewicz-Pieńkowska, K.; Jamrógiewicz, M.; Szymkowska, K.; Krenczkowska, D. Direct Human Contact with Siloxanes (Silicones)—Safety or Risk Part 1. Characteristics of Siloxanes (Silicones). Front. Pharmacol. 2016, 7, 132.
- (27) Rios, S.; Petersen, M. A.; Arps, J. H. Tandem Delivery Platform for Small Molecules and Biologic Pharmaceuticals Via Silicone Foam. *J. Med. Device* **2016**, *10* (2), 020918.
- (28) Fink, J. K. Reactive Polymers: Fundamentals and Applications: A Concise Guide to Industrial Polymers; William Andrew: 2017.

- (29) Zaki, M. F.; Tawfik, S. M. Synthesis, Surface Properties and Antimicrobial Activity of Some Germanium Nonionic Surfactants. *J. Oleo Sci.* **2014**, *6*3 (9), 921–931.
- (30) Khan, M. F.; Zepeda-Velazquez, L.; Brook, M. A. Tunable, Antibacterial Activity of Silicone Polyether Surfactants. *Colloids Surf.*, B 2015, 132, 216–224.
- (31) Gavazzoni Dias, M. F. R. Hair Cosmetics: An Overview. *Int. J. Trichology* **2015**, 7 (1), 2–15.
- (32) Hofmann, R.; Vlatković, M.; Wiesbrock, F. Fifty Years of Hydrosilylation in Polymer Science: A Review of Current Trends of Low-Cost Transition-Metal and Metal-Free Catalysts, Non-Thermally Triggered Hydrosilylation Reactions, and Industrial Applications. *Polymers (Basel, Switz.)* **2017**, *9* (12), 534.
- (33) Kunieda, H.; Uddin, M.. H.; Horii, M.; Furukawa, H.; Harashima, A. Effect of Hydrophilic- and Hydrophobic-Chain Lengths on the Phase Behavior of A—B-type Silicone Surfactants in Water. J. Phys. Chem. B 2001, 105, 5419.
- (34) So, H.; Fawcett, A. S.; Sheardown, H.; Brook, M. A. Surface-Active Copolymer Formation Stabilizes PEG Droplets and Bubbles in Silicone Foams. *J. Colloid Interface Sci.* **2013**, 390 (1), 121–128.
- (35) Kodibagkar, V. D.; Wang, X.; Pacheco-Torres, J.; Gulaka, P.; Mason, R. P. Proton Imaging of Siloxanes to Map Tissue Oxygenation Levels (PISTOL): A Tool for Quantitative Tissue Oximetry. *NMR Biomed.* **2008**, 21 (8), 899–907.
- (36) Gulaka, P. K.; Rastogi, U.; McKay, M. A.; Wang, X.; Mason, R. P.; Kodibagkar, V. D. Hexamethyldisiloxane-based Nanoprobes for ¹H MRI Oximetry. *NMR Biomed.* **2011**, *24* (10), 1226–1234.
- (37) Liu, V. H.; Vassiliou, C. C.; Imaad, S. M.; Cima, M. J. Solid MRI Contrast Agents for Long-Term, Quantitative in Vivo Oxygen Sensing. *Proc. Natl. Acad. Sci. U. S. A.* **2014**, *111* (18), 6588–6593.
- (38) Kodibagkar, V. D.; Cui, W.; Merritt, M. E.; Mason, R. P. Novel ¹H NMR Approach to Quantitative Tissue Oximetry Using Hexamethyldisiloxane. *Magn. Reson. Med.* **2006**, *55* (4), 743–748.
- (39) Agarwal, S.; Gulaka, P. K.; Rastogi, U.; Kodibagkar, V. D. More Bullets for PISTOL: Linear and Cyclic Siloxane Reporter Probes for Quantitative 1H MR Oximetry. *Sci. Rep.* **2020**, *10* (1), 1399.
- (40) Addington, C. P.; Cusick, A.; Shankar, R. V.; Agarwal, S.; Stabenfeldt, S. E.; Kodibagkar, V. D. Siloxane Nanoprobes for Labeling and Dual Modality Functional Imaging of Neural Stem Cells. *Ann. Biomed. Eng.* **2016**, *44* (3), 816–827.
- (41) Menon, J. U.; Gulaka, P. K.; McKay, M. A.; Geethanath, S.; Liu, L.; Kodibagkar, V. D. Dual-Modality, Dual-Functional Nanoprobes for Cellular and Molecular Imaging. *Theranostics* **2012**, 2 (12), 1199.
- (42) Jennings, M. C.; Minbiole, K. P. C.; Wuest, W. M. Quaternary Ammonium Compounds: An Antimicrobial Mainstay and Platform for Innovation to Address Bacterial Resistance. *ACS Infect. Dis.* **2015**, 1 (7), 288–303.
- (43) Gao, D.; Li, Y.; Lyu, B.; Jin, D.; Ma, J. Silicone Quaternary Ammonium Salt Based Nanocomposite: A Long-Acting Antibacterial Cotton Fabric Finishing Agent with Good Softness and Air Permeability. *Cellulose* **2020**, 27 (2), 1055–1069.
- (44) Lindner, M.; Bäumler, M.; Stäbler, A. Inter-Correlation among the Hydrophilic–Lipophilic Balance, Surfactant System, Viscosity, Particle Size, and Stability of Candelilla Wax-Based Dispersions. *Coatings* **2018**, *8* (12), 469.
- (45) Tong, B.; Zhang, B.; Hu, J.; Dai, R.; Deng, Y. Synthesis and Characterization of Side-Chain Liquid-Crystalline Ionomers Containing Quaternary Ammonium Salt Groups. *J. Appl. Polym. Sci.* **2003**, *90* (11), 2879–2886.
- (46) Chung, D.; Lim, J. C. Study on the Effect of Structure of Polydimethylsiloxane Grafted with Polyethyleneoxide on Surface Activities. *Colloids Surf., A* **2009**, 336 (1–3), 35–40.
- (47) Lin, L.-H.; Wang, C.-C.; Chen, K.-M.; Lin, P.-C. Synthesis and Physicochemical Properties of Silicon-Based Gemini Surfactants. *Colloids Surf.*, A **2013**, 436, 881–889.
- (48) Dragan, S.; Cazacu, M.; Toth, A. Ionic Organic/Inorganic Materials. I. Novel Cationic Siloxane Copolymers Containing Quaternary Ammonium Salt Groups in the Backbone. *J. Polym. Sci., Part A: Polym. Chem.* **2002**, *40* (21), 3570–3578.

I

- (49) Hooper, R.; Lyons, L. J.; Mapes, M. K.; Schumacher, D.; Moline, D. A.; West, R. *Macromolecules* **2001**, 34, 931.
- (50) Berry, J. D.; Neeson, M. J.; Dagastine, R. R.; Chan, D. Y. C.; Tabor, R. F. Measurement of Surface and Interfacial Tension Using Pendant Drop Tensiometry. *J. Colloid Interface Sci.* **2015**, 454, 226–237
- (51) Provencher, S. W. A Constrained Regularization Method for Inverting Data Represented by Linear Algebraic or Integral Equations. *Comput. Phys. Commun.* **1982**, *27* (3), 213–227.
- (52) Scotti, A.; Liu, W.; Hyatt, J. S.; Herman, E. S.; Choi, H. S.; Kim, J. W.; Lyon, L. A.; Gasser, U.; Fernandez-Nieves, A. The CONTIN Algorithm and Its Application to Determine the Size Distribution of Microgel Suspensions. *J. Chem. Phys.* **2015**, *142* (23), 234905.
- (53) Zhu, X.; Shen, J.; Liu, W.; Sun, X.; Wang, Y. Nonnegative Least-Squares Truncated Singular Value Decomposition to Particle Size Distribution Inversion from Dynamic Light Scattering Data. *Appl. Opt.* **2010**, *49* (34), 6591.
- (54) rilt File Exchange MATLAB Central.
- (55) Hansen, P. C. Regularization Tools Version 4.0 for Matlab 7.3. Numer. Algorithms 2007, 46 (2), 189–194.
- (56) Nakajima, Y.; Shimada, S. Hydrosilylation Reaction of Olefins: Recent Advances and Perspectives. *RSC Adv.* **2015**, *5* (26), 20603–20616.
- (57) Murthy, R.; Shell, C. E.; Grunlan, M. A. The Influence of Poly (Ethylene Oxide) Grafting via Siloxane Tethers on Protein Adsorption. *Biomaterials* **2009**, *30* (13), 2433–2439.
- (58) Geetha, B.; Mandal, A. B.; Ramasami, T. Synthesis, Characterization, and Micelle Formation in an Aqueous Solution of Methoxypolyethylene Glycol Macromonomer, Homopolymer, and Graft Copolymer. *Macromolecules* **1993**, *26* (16), 4083–4088.
- (59) Szutkowski, K.; Kołodziejska, Ż.; Pietralik, Z.; Zhukov, I.; Skrzypczak, A.; Materna, K.; Kozak, M. Clear Distinction between CAC and CMC Revealed by High-Resolution NMR Diffusometry for a Series of Bis-Imidazolium Gemini Surfactants in Aqueous Solutions. *RSC Adv.* **2018**, *8* (67), 38470–38482.